RNA (2000), *6*:206–219. Cambridge University Press. Printed in the USA.

A tertiary interaction detected in a human U2-U6 snRNA complex assembled in vitro resembles a genetically proven interaction in yeast

SABA VALADKHAN and JAMES L. MANLEY
Department of Biological Science, Columbia University, New York, New York 10027, USA

ABSTRACT

U2 and U6 small nuclear RNAs are thought to play critical roles in pre-mRNA splicing catalysis. Genetic evidence suggests they form an extensively base-paired structure within the spliceosome that is required for catalysis. Especially in light of significant similarities with group II self-splicing introns, we wished to investigate whether the purified RNAs might by themselves be able to form a complex similar to that which appears to exist in the spliceosome. To this end, we synthesized and purified large segments of human U2 and U6 snRNAs. Upon annealing, the two RNAs efficiently formed a stable and apparently extensively base-paired (T_m = 50–60 °C in the presence of 20 mM Mg^{2+}) complex. To investigate possible tertiary interactions, we subjected the annealed complex to UV irradiation, and two crosslinked species were identified and characterized. The major one links the second G in the highly conserved and critical ACAGAGA sequence in U6 with an A in U2 just 5′ to U2-U6 helix Ia and opposite the invariant AGC in U6. Remarkably, this crosslink indicates a tertiary interaction essentially identical to one detected previously by genetic covariation in yeast. Together our results suggest that purified U2 and U6 snRNAs can anneal and fold to form a structure resembling that likely to exist in the catalytically active spliceosome.

Keywords: pre-mRNA splicing; tertiary interaction; UV crosslinking; U2-U6 complex

INTRODUCTION

Removal of introns from eukaryotic mRNA precursors is carried out by the spliceosome, a complex and dynamic assembly containing five major small nuclear RNA molecules and a large number of proteins (for reviews, see Kramer, 1996; Burge et al., 1999; Kambach et al., 1999). Genetic suppression studies, in vitro functional assays, and crosslinking data have provided evidence for the existence of extensive RNA–RNA interactions between both the snRNAs and the pre-mRNA and the snRNAs themselves (reviewed by Nilsen, 1998; Staley & Guthrie, 1998). Assembly and activation of the spliceosome can be viewed as a stepwise procedure involving multiple RNA–RNA interactions. The first stage involves recognition of the 5′ splice site and the branch site through base-pairing interactions with U1 and U2 snRNAs, respectively, followed by the entry of U4/U6.U5 snRNAs as a tripartite preassembled complex. Through a series of protein-mediated conformational changes, U6 snRNA replaces U1 at the 5′ splice site, accompanied by unwinding of the U4-U6 base-paired complex. At the same time, U6 and U2 become base paired, positioning the 5′ splice site and the branch site close to each other. Through two consecutive transesterification reactions, the 3′ and 5′ exons are joined together and the intron is released as a branched (lariat) molecule. As the conserved loop I of U5 seems to be dispensable for the first step of catalysis in yeast (O'Keefe et al., 1996), and for both the first and the second steps in mammalian extracts (Segault et al., 1999), it is likely that U2 and U6 form the major catalytic RNA domains at the active site of the spliceosome.

The most conserved of the spliceosomal snRNAs, U6 snRNA, is thought to play an important role in splicing catalysis. Mutagenesis data in yeast and human suggest an important catalytic role for two extremely conserved regions in U6 (the ACAGAGA and AGC sequences, see Fig. 1). Several point mutations in these regions lead to either total loss of splicing activity or a block after the first step (Fabrizio & Abelson, 1990; Madhani et al., 1990; Wolff et al., 1994). Similarly, thiophosphate substitutions in the backbone phosphates upstream of two of the nucleotides in the ACA**G**AG**A**

Reprint requests to: James L. Manley, Department of Biological Science, Columbia University, New York, New York 10027, USA; e-mail: jlm2@columbia.edu.

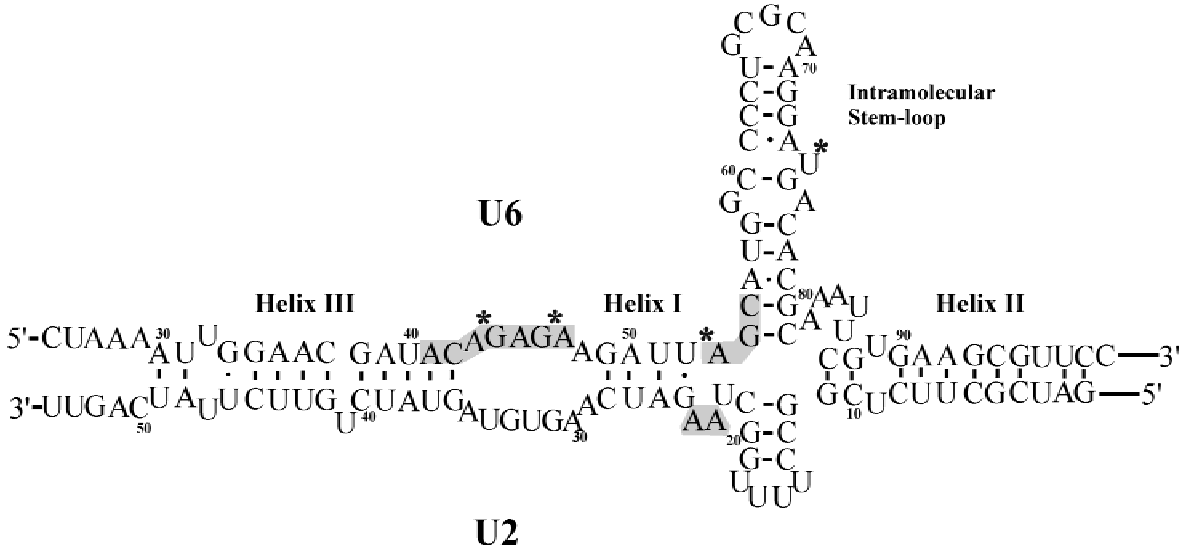

FIGURE 1. The proposed base-pairing interactions between the central domains of human U2 and U6. The base-paired helices I, II, and III and the intramolecular stem-loop of U6 are shown. Sites of catalytically important nonbridging phosphate oxygen atoms are marked by asterisks. The shaded boxes mark the invariant regions in U6 and the 2-nt bulge in U2. Numbers indicate nucleotide positions from the 5′ end.

sequence, the first nucleotide of the invariant **A**GC and a nucleotide located at the bulge of the intramolecular helix of U6 (Fig. 1), either totally abolished or reduced splicing activity, or led to a block before the second step (Fabrizio & Abelson, 1992; Yu et al., 1995). Furthermore, crosslinking data in yeast and human have provided evidence for the proximity of U6 A45 (in the invariant ACAG**A**GA) and nucleotides close to the 5′ splice site (Sontheimer & Steitz, 1993; Kim & Abelson, 1996). In a recent study in yeast, the last nucleotide of the invariant ACAGA**G**A was found to interact with the first nucleotide of the intron, and to participate in selection of the 5′ splice site (Luukkonen & Séraphin, 1998a). Taken together, the current data is suggestive of participation of U6 in both steps of splicing, possibly by binding and coordinating catalytically important metal ions, as suggested by the phosphorothioate substitution studies.

In the active spliceosome, U6 is base paired to U2 snRNA, interacting through three base-paired helices (Fig. 1). The region downstream of the conserved ACA GAGA in U6 and upstream of the branch-binding site in U2 interact to form helix I (Madhani & Guthrie, 1992), whereas the 3′ end of U6 and 5′ end of U2 base pair in helix II (Hausner et al., 1990; Datta & Weiner, 1991; Wu & Manley, 1991). Helix III results from base pairing of sequences upstream of ACAGAGA box in U6 and downstream of the branch-binding site in U2 (Sun & Manley, 1995). These interactions may be somewhat different between yeast and mammals. For example, in yeast, helix I is divided into two helices, Ia and Ib, by a 2-nt bulge (Madhani & Guthrie, 1992, 1994b), but in mammals, the nucleotides corresponding to those in helix Ib appear to form a short intramolecular stem-loop in U2 and the proximal part of the intramolecular stem-loop in U6, which makes this stem-loop in mammals longer than its yeast counterpart (Sun & Manley, 1995; although see Fortner et al., 1994). In yeast, helix III is not essential for catalytic activity (Yan & Ares, 1996), and helix II seems to be largely redundant with helix Ib (Field & Friesen, 1996).

Several lines of evidence argue for the possibility of RNA-based catalysis in the spliceosome. The similarity between the spliceosome and group II introns is particularly intriguing. Both systems utilize the same two-step transesterification strategy for splicing, with a high similarity in both stereochemistry of catalysis and the catalytic intermediates. The catalytic domain 5 of group II introns resembles spliceosomal U6 not only in overall structure and identity of the conserved AGC sequence, which is essential for catalysis in both systems, but also seems to have similar backbone and sequence requirements (Chanfreau & Jacquier, 1994, 1996; Boulanger et al., 1995; Peebles et al., 1995; Podar et al., 1998; Podar & Perlman, 1999). The presence of interchangeable domains between snRNAs and group II introns and evidence suggesting metal ion-based catalysis in the spliceosome add further strength to the possibility that splicing might be RNA catalyzed (Steitz & Steitz, 1993; Hetzer et al., 1997; Sontheimer et al., 1997, 1999; Tuschl et al., 1998).

If the spliceosome is in fact an RNA-centric catalytic machine, its RNA components might be expected to have the potential to position and stabilize interactions between components of the active site(s). Evidence for one such interaction comes from several studies de-

scribing direct or indirect interactions between the 2-nt bulge region in U2 (located downstream of the short 5′ U2 intramolecular helix in human and between helices Ia and Ib in yeast, see Fig. 1) and the conserved ACAGAGA box of U6. A genetic covariation study in yeast provided evidence for a tertiary interaction between G46 in the conserved ACAGA**G**A sequence in U6 and A24 in the 2-nt bulge in U2, and also suggested that this interaction might play a role in the second step of splicing (Madhani & Guthrie, 1994a). The tertiary interaction thus might contribute to formation of the active site by helping to juxtapose residues involved in catalysis.

We previously described a long-range interaction in purified U6 snRNA that positions the two conserved, functionally important regions of U6 (ACAGAGA and AGC) close to each other (Sun et al., 1998). Here we provide evidence for the existence of a tertiary interaction in a base-paired complex of purified U2 and U6 snRNAs assembled in vitro. The complex formed efficiently under appropriate conditions and was stable at physiological temperatures. Following irradiation by short UV light, two crosslinked species were detected and analyzed. Remarkably, the major crosslink was found to join conserved, catalytically important regions of U2 and U6, and to be nearly identical to the U2-U6 tertiary interaction detected genetically in yeast (Madhani & Guthrie, 1994a). The presence of the same tertiary fold in a protein-free U2-U6 RNA complex in vitro and in vivo shows that U2 and U6 snRNAs can form at least part of the structure necessary for splicing without the help of proteins, and provides additional evidence for the possibility of RNA-based catalysis in the spliceosome.

RESULTS

U2 and U6 snRNAs can efficiently form a complex in vitro

As described above, there are several secondary and tertiary interactions between U2 and U6 snRNAs that are important for splicing. Especially in light of similarities with group II self-splicing, we wished to investigate the potential of these two snRNAs to interact in vitro. To this end, the central domain of U6 snRNA (nt 25–99), which is sufficient for splicing activity in vitro (Wolff & Bindereif, 1992), and the 5′ domain of U2 snRNA (nt 1–54), which contains all the sequences known to interact with U6, were transcribed in vitro, purified, and one or the other end labeled. After mixing the two snRNAs at different concentrations (from 1 nM to 300 nM), they were renatured by heating followed by slow cooling in different buffers and analyzed on a native gel. U2 and U6 efficiently formed a complex under most conditions tested, the only requirement being gentle cooling and the presence of salt in the annealing buffer (Fig. 2A; see below). Complex formation was most efficient in the pH range 6.8–7.2 (not shown), and its efficiency increased by raising the concentration of $MgCl_2$, such that all the labeled RNA entered the complex at 100 mM $MgCl_2$ (Fig. 2B). The complex was very stable, with a T_m between 50 and 60 °C in the presence of 20 mM Mg^{2+} (Fig. 2C). The annealing likely involves extensive base pairing, as labeled U6 in the presence of excess unlabeled U2 and U6 preferentially formed a complex with U2 rather than forming a U6 homodimer (Fig. 2D), which can result from base-pairing potential involving the intramolecular helix region and sequences 5′ and 3′ to it (Sun et al., 1998; results not shown). Initially magnesium ions were used in the reaction, but sodium, ammonium, manganese, calcium, and zinc could replace magnesium in the annealing buffer, although monovalent salts were significantly less efficient in promoting annealing than were divalent salts, with very little or no complex formed when lower concentrations of monovalent salts (e.g., 100 mM) were used (Fig. 3A and data not shown). No complex formed in the absence of salt.

Two crosslinked species result from UV irradiation of the U2-U6 complex

We next probed possible tertiary interactions within the U2-U6 complex by UV crosslinking. Annealing reactions were irradiated with short wave UV for different times (see Materials and Methods) and samples were loaded on a denaturing gel (Fig. 4A). Following UV irradiation, two slow-moving bands appeared on the gel (U2-U6 XL1 and 2). Both species resulted from a crosslink between U2 and U6, as irradiating U2-U6 complexes containing either labeled U2 or U6 resulted in the appearance of identical bands (Fig. 4A, compare lanes 8 and 9 with 11 and 12). The crosslinked species formed with high efficiency, and increased in amount with longer UV exposure, with as much as 50% of the annealed U2-U6 complexes being crosslinked after 1 h of irradiation (Fig. 4A; results not shown). In addition to these two crosslinks, we also detected a band in all samples containing labeled U6 (Fig. 4A, lanes 5, 6, 11, and 12), which corresponds to the intramolecular crosslink resulting from UV irradiation of U6 in the absence of U2 (Sun et al., 1998). The U2-U6 crosslinks most likely resulted from an interaction already present in the annealed U2 and U6 complex, as when the annealed RNAs were run on a native gel before and after crosslinking, the complexes formed had identical mobility (Fig. 4B). As certain pyrimidine–pyrimidine photoadducts can undergo photoreversion upon reirradiation with UV light with a wavelength below 230 nm, we reirradiated purified crosslinked samples in an attempt to characterize the crosslink. However, no increase in the amount of uncrosslinked RNA could be detected (results not shown).

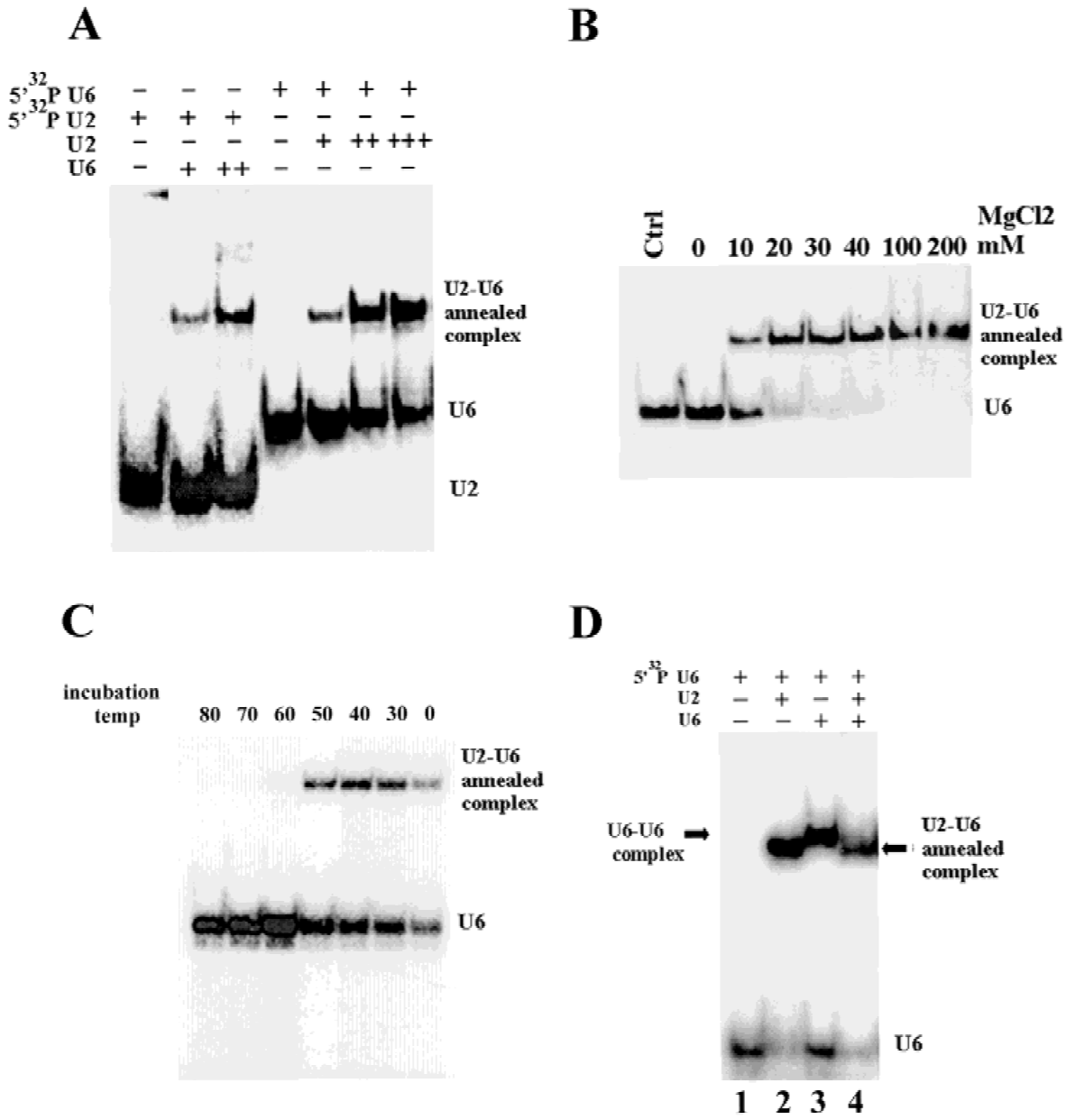

FIGURE 2. Properties of the annealed U2-U6 complex. **A**: Formation of the annealed U2-U6 complex. RNAs were annealed in a buffer containing 40 mM Tris, pH 6.8, and 40 mM $MgCl_2$ and resolved by nondenaturing PAGE. The labeled and unlabeled species present in the reaction mixture are indicated above each lane. Positions of bands representing U2, U6, and the annealed U2-U6 complex are shown to the right. All reactions contained 10 nM final concentration of the labeled RNA. Concentration of the unlabeled RNA was 1 nM, 10 nM, or 100 nM for U2 and 1 nM or 10 nM for U6. **B**: Effect of Mg^{2+} concentration on complex formation. The concentration of Mg^{2+} in the annealing buffer is indicated above each lane. The control (Ctrl) reaction contained 40 mM Mg^{2+} and labeled U6 only. All reactions contained 10 nM 5′-labeled U6 and 100 nM unlabeled U2. Locations of U6 and the U2-U6 complex in the gel are indicated to the right. **C**: T_m of the annealed complex. Preformed complexes were incubated at the indicated temperatures for 5 min, rapidly cooled on ice, and loaded on a native gel. Positions of U6 and the annealed U2-U6 complex are indicated. Each reaction contained 10 nM 5′-labeled U6 and 100 nM U2. The reaction buffer contained 20 mM $MgCl_2$. **D**: Competition of equimolar amounts of unlabeled U2 and U6 for complex formation with a limiting amount of labeled U6. The arrows point to the position of the annealed U2-U6 complex (lanes 2 and 4) and the U6 dimer (lane 3). Position of free U6 is indicated. Each reaction contained 10 nM 5′-labeled U6 and 100 nM final concentration of the unlabeled RNAs indicated above each lane.

To determine the salt requirements for the formation of the crosslink, U2 and U6 were annealed in buffers containing different salts. The concentration of the RNAs was adjusted so that annealing would result in formation of the same amount of complex in all buffers. Reaction mixtures were irradiated with UV and resolved on a denaturing gel (Fig. 3B). Crosslinking was significantly less efficient when NaCl and NH_4Cl were the

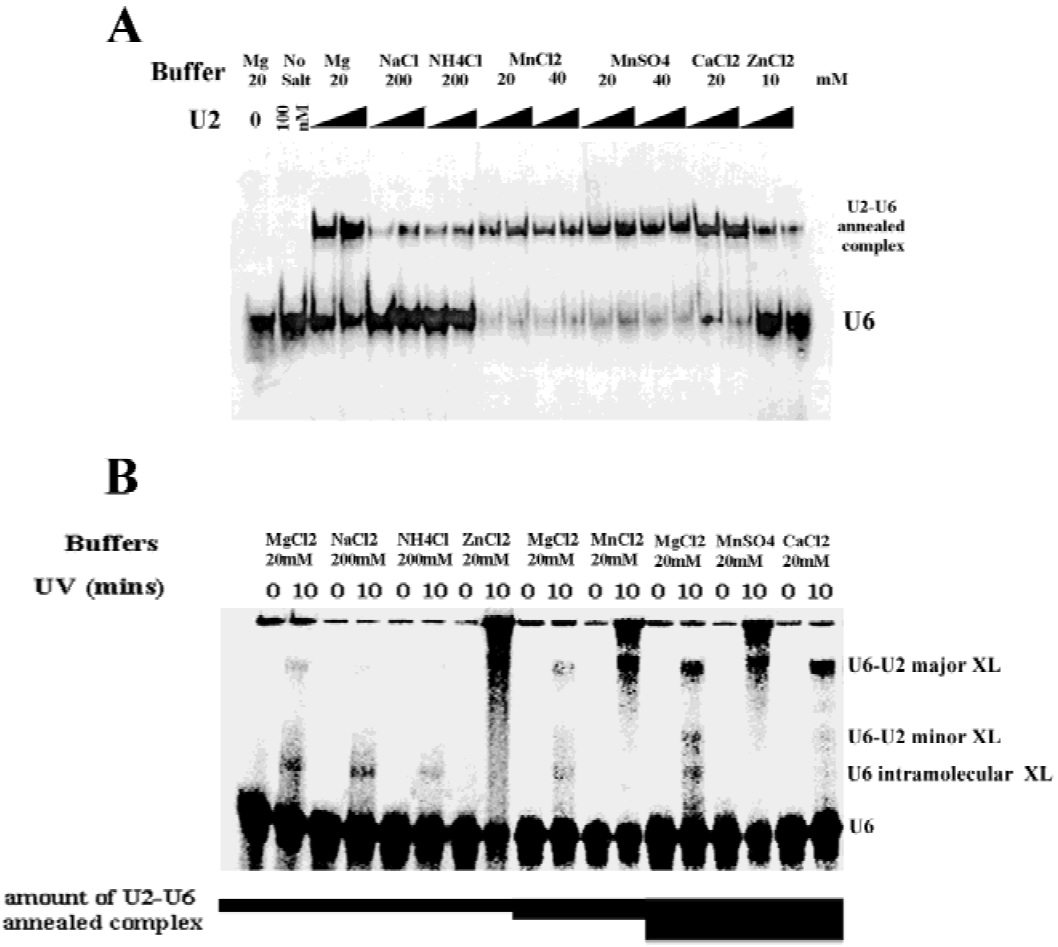

FIGURE 3. Ionic requirements for complex formation and crosslinking. **A**: Effect of different salts on formation of the U2-U6 complex. For each salt tested, two different concentrations of unlabeled U2 were added (50 nM and 300 nM). All reactions contained 10 nM 5′-labeled U6. The concentration of each cation in the annealing mixture is indicated above each lane. Positions of U6 and the U2-U6 complex are indicated on the right. **B**: Effect of different salts on crosslinking. Crosslinking was performed in buffers containing each cation at the indicated concentration. All reactions contained 10 nM 5′-labeled U6. U2 concentrations were adjusted so that the same amount of the U2-U6 base-paired complex formed in the lanes underlined with black bars of the same width. Samples were taken before (time point 0) and after 10 min of UV irradiation. Location of the major and minor U2-U6 crosslinked product, the U6 intramolecular crosslinked product, and uncrosslinked U6 are indicated on the right.

only salts in the buffer, but was slightly more efficient when $MnCl_2$, $MnSO_4$, or $CaCl_2$ were used instead of $MgCl_2$. The ionic requirements for crosslinking are thus similar to those for complex formation.

Mapping the location of the crosslinked nucleotides using oligo-directed RNase H digestion

We employed oligo-mediated RNase H digestion to determine the approximate location of the crosslinked residue(s). DNA oligos complementary to different regions of U2 and U6 were used to target the RNAs for RNase H digestion. The crosslinked species, labeled at either end of U6 or U2, were purified from a denaturing gel and annealed to the complementary oligos. After annealing, RNase H was added and samples were taken at different time points. Parallel reactions were set up using uncrosslinked, similarly labeled U2 or U6.

First, we set out to determine the site of the crosslinked nucleotides in the major crosslinked product using two sets of oligos complementary to U2 and U6 (Fig. 5). For U6, we used oligos complementary to the 5′ end (nt 25–42), the central region (nt 37–55), the 5′ (nt 50–71) and 3′ (nt 67–82) side of the intramolecular stem-loop, and the 3′ end (nt 82–99). When the oligo complementary to the middle part of U6 (oligo 37–55) was used for RNase H targeting of a crosslinked product carrying a 5′-end labeled U6, a new band appeared that migrated much faster than U6 on the gel (Fig. 5A, left panel). The fragment had the same mobility as the fragment resulting from RNase H digestion of uncrosslinked 5′-labeled U6, which corresponds to nt 25–36 of U6. For this fragment to be released from the crosslink,

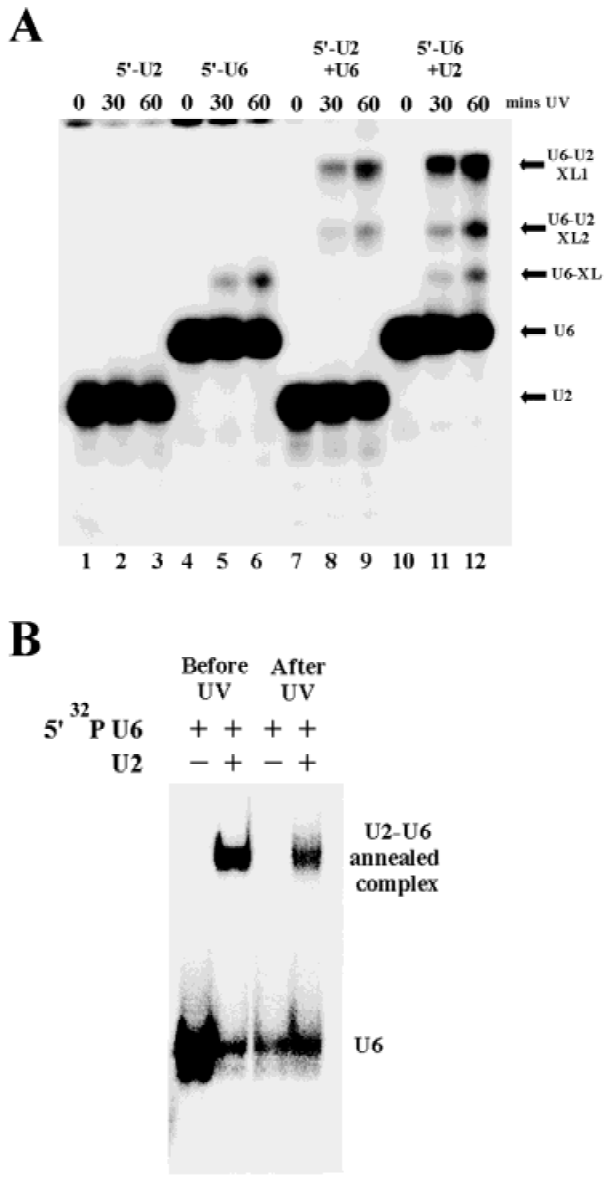

FIGURE 4. UV crosslinking of the U2-U6 complex. **A**: Formation of the U2-U6 crosslinked species. Reaction mixtures containing 5′-labeled U2 (lanes 1–3), 5′ U6 (lanes 4–6), 5′ U2 and unlabeled U6 (lanes 7–9), and 5′ U6 and unlabeled U2 (lanes 10–12) were annealed and irradiated with short UV for the indicated length of time. Positions of the intramolecular U6 crosslink (U6-XL, lanes 5, 6, 11, 12; see Sun et al., 1998), the two crosslinked species containing both U2 and U6 (U6-U2 XL1 and XL2), and uncrosslinked U2 and U6 are indicated to the right. Each reaction contained 10 nM of the labeled RNA and 100 nM final concentration of the unlabeled RNA. **B**: Effect of UV irradiation on migration of the annealed U2-U6 complex through a nondenaturing gel. Samples were taken before and after 30 min of irradiation with short UV and resolved by native PAGE. All reactions contained 10 nM 5′-labeled U6. In those reactions that contained U2, the final U2 concentration was 100 nM. Positions of the U2-U6 annealed complex and free U6 are shown on the right.

the crosslinked residues must be located downstream of nt 36. The same reaction was repeated, this time with a 3′ U6-U2 crosslink. A new band appeared that migrated at the same position as the U6 fragment 56–99 resulting from an identical RNase H reaction on uncrosslinked 3′ U6 (Fig. 5A, right panel), proving that the crosslinked nucleotides are 5′ to nt 56 in U6, narrowing the location of the crosslinked nucleotides to nt 37–55 in U6. The results obtained with other oligos supported this conclusion (data not shown).

The same procedure was repeated for crosslinked species containing 5′ or 3′-labeled U2 snRNA (Fig. 5B). Most informative were the results obtained with an oligo complementary to nt 14–36 of U2. When this oligo was used with a crosslinked species containing 5′-labeled U2, a short fragment comigrating with U2 fragment 1–13, resulting from RNase H digestion of uncrosslinked 5′ U2, was observed (Fig. 5B, right panel). The fragment released by this oligo from 3′ U2-containing crosslinks also had similar mobility to fragments released from uncrosslinked 3′ U2 (Fig. 5B, left panel). These data show that the crosslinked nucleotide(s) are located in the region complementary to this oligo, that is, between nt 14 and 36 of U2, which encompasses the branch point binding site and the region upstream of it.

Using the same approach, the approximate location of the crosslinked nucleotides in the minor U2-U6 crosslinked species was determined. An oligo that targeted nt 28–42 in U2 resulted in the appearance of a band that migrated slightly faster than the original 3′ U2-U6 crosslink (Fig. 5C, right panel). This result locates the crosslinked nucleotide(s) downstream of the region targeted by this oligo (3′ to nt 42 in U2). A 3′ U6-U2 crosslink targeted by U6 oligo 25–42, which anneals to the 5′ end of U6, resulted in the appearance of a fragment that comigrated with the fragment released from an uncrosslinked 3′ U6, which is consistent with the crosslink being at the 5′ end of the molecule (Fig. 5C, left panel). The sequences crosslinked in the minor product, the 5′ end of U6 and the 3′ end of U2, are capable of extensive base-pairing interactions, forming helix III in mammals (Sun & Manley, 1995).

The bases juxtaposed by the major crosslink are located in highly conserved regions of U2 and U6

We next used limited alkaline hydrolysis to map more precisely the location of crosslinked nucleotides. U2 or U6 was labeled at either end and used for crosslinking. The gel-purified crosslinked product was subjected to alkaline hydrolysis and loaded on a denaturing gel along with an RNase T1 digestion reaction to help determine the site of the stops. The hydrolysis ladder will stop before the crosslinked nucleotide, as hydrolysis of the phosphodiester bonds after this nucleotide will not result in release of a labeled fragment.

To determine the sites of the major crosslink, we first purified a crosslinked product containing 5′-labeled U6. The hydrolysis ladder resulting from this crosslink showed a stop immediately before G46, in the invariant ACAGA**G**A box (Fig. 6A). This result is consistent with

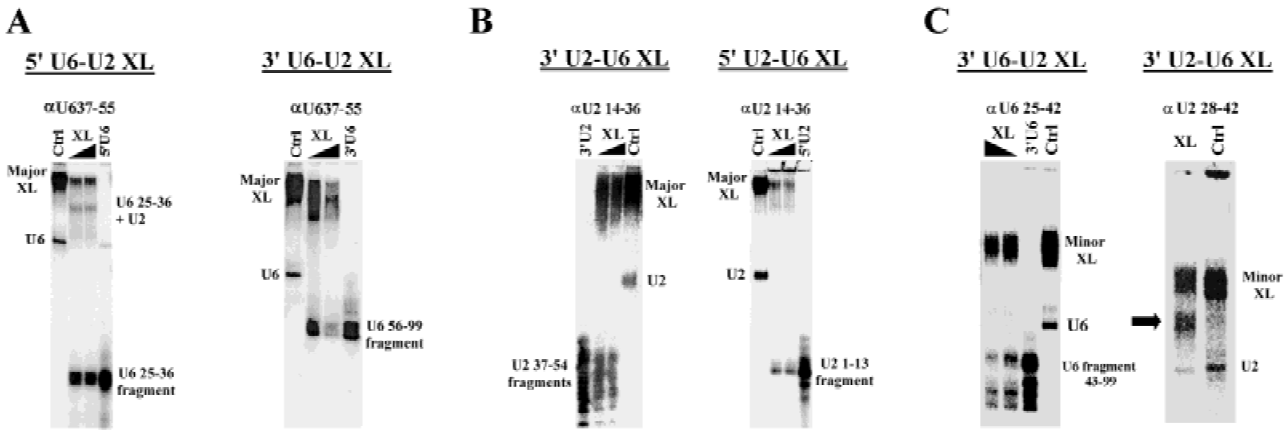

FIGURE 5. Mapping of crosslinked nucleotides by oligonucleotide-mediated RNase H digestion. Crosslinked RNAs were labeled at the 3′ or 5′ end of U2 or U6 and annealed to oligos complementary to different regions of U2 or U6. For each oligo, a parallel reaction was performed on similarly labeled, uncrosslinked U2 or U6 (lanes marked 3′/5′ U2/U6 in each panel). Lanes marked XL represent time course of RNase H digestion of the U2-U6 crosslinked species. For each panel, the labeled crosslinked species analyzed is shown in underlined letters at the top, with the labeled RNA indicated first. For each set of experiments, a control reaction was performed in which no oligo was added to the reaction mixture (lanes marked Ctrl). Positions of the crosslinked species (Major/Minor XL), uncrosslinked U2 or U6, and fragments released as a result of RNase H digestion are indicated at the side of each panel. **A**: RNase H digestion of the major crosslinked species labeled at the 5′ (left panel) or 3′ (right panel) end of U6, with an oligo complementary to nt 37–55 of U6 (αU6 37–55). The band labeled U6 25–36+U2 results from the simultaneous presence of a second crosslinked site in the region of helix III (similar to that in the minor crosslinked species) in a subset of the major crosslinked products (see text). **B**: RNase H reactions performed on crosslinked species labeled at the 3′ (left) or 5′ (right) end of U2. The oligo used targets nt 14–36 of U2 (αU2 14–36). **C**: Determination of the approximate location of the crosslinked nucleotides in the minor crosslinked species. **Left**: Minor crosslinked species labeled at the 3′ end of U6, targeted for RNase H digestion by an oligo complementary to nt 25–42 of U6 (αU6 25–42). **Right**: RNase H digestion of the 3′-U2-labeled minor crosslinked product using an oligo which anneals to nt 28–42 of U2 (αU2 28–42). Arrow points to the new band resulting from the RNase H reaction.

the RNase H data, which located the crosslinked nucleotides between nt 37–55. The same approach was next used to map the crosslinked nucleotide(s) in U2. The major crosslinked species containing 5′-labeled U2 was isolated and subjected to gentle hydrolysis. A stop in the hydrolysis ladder before nucleotide A23 in U2 was observed (Fig. 6B). This nucleotide is located in a highly conserved region, in the 2-nt bulge upstream of helix I in U2. To confirm these results, we performed alkaline hydrolysis on crosslinked species containing 3′-labeled U2 or U6. The results (not shown) were entirely consistent with the 5′-labeled crosslinks, and in addition proved that the major U2-U6 crosslink resulted from photoadduction at a single location. Remarkably, the interaction captured by the major crosslink is very similar to the genetic tertiary interaction described in yeast by Madhani and Guthrie (1994a).

The minor crosslinked species adjoins the 5′ end of U6 and the 3′ end of U2

Similarly, we employed alkaline hydrolysis to determine the location of the crosslinked nucleotides in the minor crosslinked species. When a crosslink containing 5′ U2-U6 was hydrolyzed, the ladder stopped before nt U47 (Fig. 6C), consistent with the results of the RNase H studies described above. We were unable to map the crosslinked nucleotide in U6 in the minor crosslinked species using this approach due to technical problems, so we instead mapped the crosslink by primer extension. A primer annealing to the 3′ end of U6 (nt 82–99) was used in reverse transcription reactions with both minor and major crosslinked species as templates. The results (Fig. 6D) support the presence of the crosslinked nucleotide(s) at the 5′ end of U6, mapping it to the region around nt 29–32 in U6. This region is located in proximity of U47 in U2 in helix III, further supporting the presence of this helix in the U2-U6 annealed complex. Under certain conditions, we were able to obtain a minor fraction of crosslinked products which harbored both of the crosslinks described above, proving that the interaction between G46 of U6 and A23 of U2 and the base-pairing interaction in the region of helix III are not mutually exclusive (for example, see Fig. 5A, left panel, and our unpubl. data).

The interaction captured by the crosslink is not dependent on the identity of the crosslinked nucleotides

We next wished to determine if mutations in one of the nucleotides involved in the crosslink affect either complex formation or crosslinking. The nucleotide crosslinked in U6, G46, was therefore mutated to all of the other three bases and the resultant RNAs were used for annealing and crosslinking. Remarkably, following

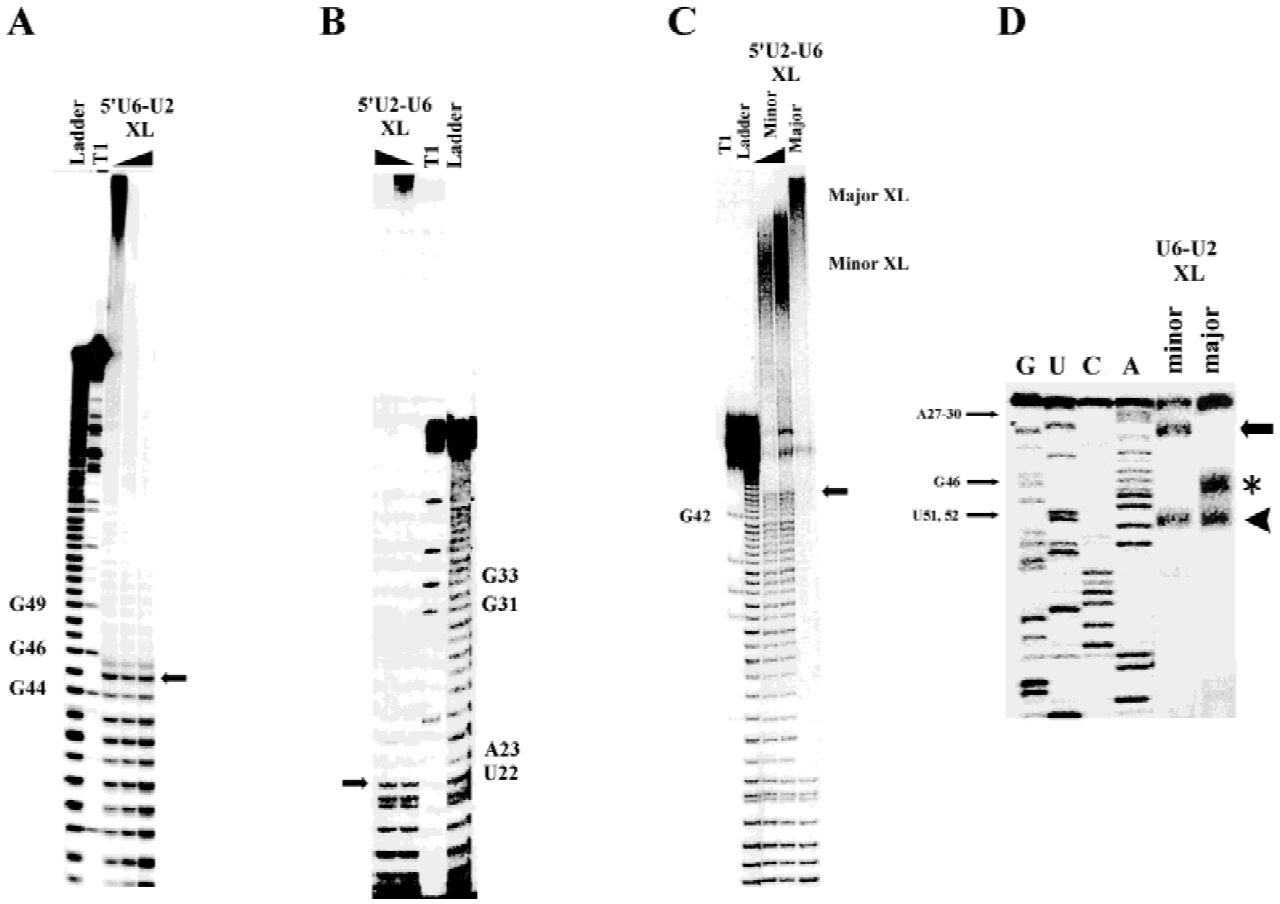

FIGURE 6. Identification of the crosslinked residues in the major and minor U2-U6 crosslinked products. Limited alkaline hydrolysis of the crosslinked species labeled at one or the other end of U2 or U6. Parallel reactions were performed on similarly labeled uncrosslinked RNAs (lanes marked as ladder). Reaction mixtures were loaded on denaturing gels along with RNase T1 digestion ladders (lanes labeled T1). Arrows point to the site of stops in the hydrolysis ladders. Identity of nucleotides on the sequencing ladders is indicated at the side of each panel. **A**: Ladders resulting from limited alkaline hydrolysis of the major crosslinked product labeled at the 5′ end of U6 (5′ U6-U2 XL). **B**: Alkaline hydrolysis reactions performed on 5′ U2-labeled major crosslinked species (5′ U2-U6 XL). **C**: Alkaline hydrolysis of the major and minor crosslinked species (5′ U2-U6 XL, major and minor) labeled at the 5′ end of U2, run side by side. **D**: Mapping the site of crosslinked nucleotides using primer extension. Unlabeled major and minor crosslinked species (U6-U2 XL, major and minor) were annealed to an oligonucleotide complementary to the 3′ end of U6, along with appropriate sequencing reactions (lanes marked G, U, C, and A). Arrowhead, asterisk, and thick arrow mark the locations of the stops, with the stop marked by the arrowhead likely resulting from an intramolecular crosslinking event. Locations of the relevant nucleotides are marked on the sequencing ladders (thin arrows).

irradiation of the mutant U6-U2 complexes, crosslinked species with mobilities similar to wild-type U6-U2 crosslink formed with equal efficiency with all three mutant RNAs (Fig. 7A).

To determine whether the site of crosslinking changed in the mutant RNAs, we performed alkaline hydrolysis on the purified crosslinked species. The results revealed in each case a difference in the identity of the U6 residue crosslinked (Fig. 7B). The mutant U6 G46A RNA was predominantly crosslinked at A45, the nucleotide adjacent to the normal site. Mutants G46U and G46C, however, were each crosslinked at a more distal residue, U52. These results indicate that U6 G46 is not essential for the U2-U6 crosslinking, and, at least in the case of G46A, the interaction is likely to be very similar to that in wild type.

DISCUSSION

We have used in vitro-synthesized human U2 and U6 snRNAs in an attempt to reconstitute a U2-U6 complex resembling that formed in the active spliceosome, with the aim of determining first whether the purified RNAs could form such a complex, and second whether the interactions involved would be similar to those thought to occur in vivo. Indeed, we found that a stable complex resulting from the annealing of the two RNAs formed efficiently under most tested conditions, the only requirement for its formation being the presence of salts in the annealing buffer. Two interactions captured by UV crosslinking of the U2-U6 annealed complex paralleled interactions demonstrated in vivo by genetic suppression studies (Madhani & Guthrie, 1994a; Sun & Manley, 1995).

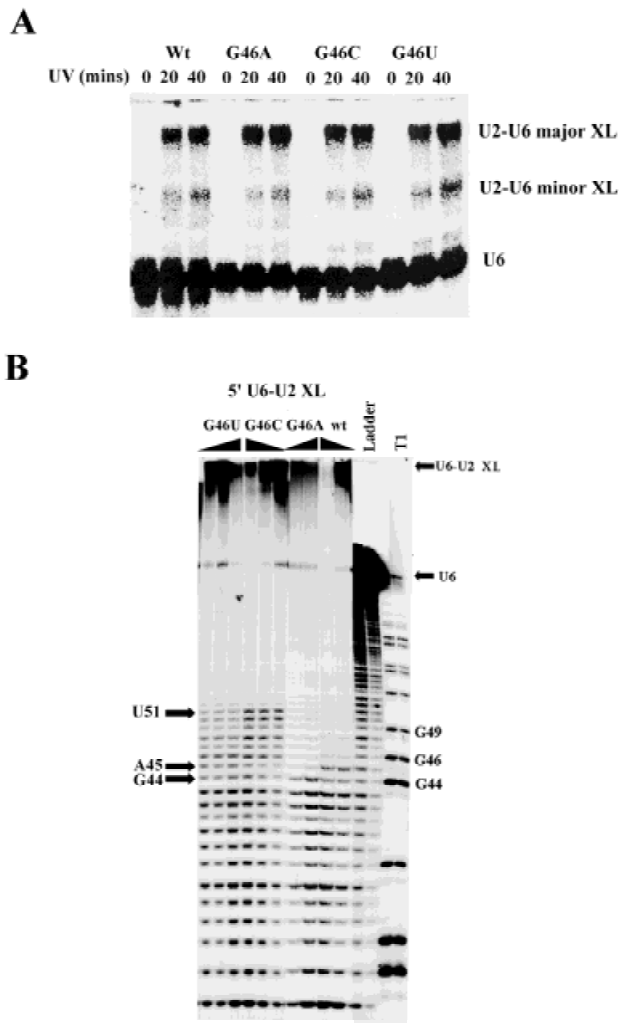

FIGURE 7. Effect of mutations of the crosslinked nucleotides on formation of the major crosslink. **A**: Effect of point mutations in U6 G46 on formation of the crosslink. Wild-type (Wt) and mutant (G46A, G46C, and G46U) U6 RNAs were annealed to wild-type U2 and irradiated with short UV for the indicated lengths of time. All reactions contained 10 nM 5′ U6 and 100 nM unlabeled U2. Locations of the major and minor crosslinked species (U2-U6 major and minor XL) and uncrosslinked U6 are shown on the right. **B**: Mapping the location of crosslinked nucleotides in the major crosslinked products carrying mutant U6 RNAs. Major crosslinked products obtained from mutant U6 RNAs (G46A, G46C, and G46U) were subjected to alkaline hydrolysis for 3, 4, and 5 min, along with crosslinked species carrying wild-type U6 (wt). Arrows point to the location of the stops. Ladder: Hydrolysis ladder of uncrosslinked 5′ U6. T1: RNase T1 digestion of uncrosslinked 5′ U6. Positions of uncrosslinked U6, the unhydrolyzed major crosslinked product (U2-U6 XL), and nucleotides on the sequencing ladder are indicated to the right.

The U2-U6 annealed complex: Similarities with the complex in the active spliceosome?

U2 and U6 have extensive base-pairing potential, being complementary in at least two extended regions (helices II and III, Fig. 1). The possibility of the existence of the same base-pairing interactions in our system is strengthened by the location of the minor UV-crosslinked species, which juxtaposes nucleotides located across the base-paired helix III. The high stability and T_m of the complex also provides evidence for its being optimally base paired, and indeed the optimal secondary structure of a complex between U2 and U6 as determined by computer analysis (RNAstructure, version 3.2) is almost identical to the structure proved by genetic complementation studies and depicted in Figure 1 (our unpubl. data). Helix I, unlike helices II and III, lacks an extended base-pairing potential, but as the regions base paired in helix I can be held in the proper alignment by helix III in our U2-U6 complex, it is plausible to hypothesize that helix I exists in the complex, and indeed psoralen crosslinking studies point to the existence of helices I, II, and III in the U2-U6 annealed complex (our unpubl. data). The possibility that the U2-U6 annealed complex might be identical or very similar to the structure formed in vivo is tantalizing, as it indicates the competence of the two RNA molecules to form the structure found in the spliceosome without the help of proteins.

Formation of the U2-U6 complex was dependent on heat denaturation of the reaction mixture. This requirement probably results from the stable secondary structure of U6, brought about by the potential of the sequences at the 3′ and central region of U6 to form a base-paired helix. In a previous study, it was shown that the U4–U6 base-paired complex is inherently unstable, due to the ability of U6 to form a stable intramolecular helix (Brow & Vidaver, 1995). We have determined the secondary structure of human U6 snRNA in solution using a battery of chemical modification methods and our results are consistent with the existence of a stable base-paired helix between the 3′ end of U6 and the sequences upstream of the ACA GAGA box (our unpubl. data). In vivo U6 is base paired to U4 before forming the base-paired helices with U2, but it is possible that formation of the U2-U6 complex can occur spontaneously at physiological temperatures, with U2 replacing U4 as a more stable base-pairing partner. Our data, showing the preference of U6 to enter a complex with U2 rather than forming a U6 dimer, strengthens this possibility. In a study on the stability of the U4-U6 complex (Brow & Vidaver, 1995), the T_m of the human U4-U6 complex showed a considerable increase after removal of 22 nt from the 3′ end of U6, which includes nucleotides that take part in the base-paired helix II in the U2-U6 complex. Similarly, formation of the U2-U6 complex was less efficient with a U6 RNA containing sequences 25–106 compared to U6 25–99 (our unpubl. data). These observations make it possible that the stability of the U4–U6 complex, and thus the timing of progression of spliceosome assembly by release of U6 from the U4-U6 complex and its annealing to U2, could be regulated by factors that bind to and control the availability of the 3′-end sequences in U6 for base-pairing interactions.

The major crosslinked species captures an interaction known to occur in the spliceosome

The similarity between the interaction captured in the major crosslinked species in our system and a tertiary interaction observed in vivo in a genetic covariation-suppression study in yeast by Madhani and Guthrie (1994a) is striking (see Fig. 8). Both interactions involve G46 from the conserved ACAGA**G**A sequence in U6 and the 2-nt bulge region in U2, regions which seem likely to play especially important roles in catalysis. In yeast, the interaction was shown to be important in the second catalytic step of splicing, probably due to the potential of this interaction to position the groups involved in the second step of splicing. The ACAGA**G**A box in U6, and G46 in particular, has been shown to interact with both 3′ and 5′ splice sites by genetic suppression studies (Lesser & Guthrie, 1993; Luukkonen & Séraphin, 1998a). Mutations in G46 have been shown to be incompatible with viability in yeast, due to a dramatic impairment in the second step of splicing (Fabrizio & Abelson, 1990; Madhani et al., 1990; Wolff et al., 1994). The 2-nt bulge of U2 has been crosslinked to the first nucleotide of the 3′ exon in yeast (Newman et al., 1995), and implicated in an interaction with the 5′ splice site (Luukkonen & Séraphin, 1998b). Although point mutations at this region do not have a severe phenotype, they cause a detectable increase in the level of splicing intermediates (Madhani & Guthrie, 1992, 1994a), probably by reducing the efficiency of the second splicing step. In the context of mutations in G46 in U6, mutations in the 2-nt bulge of U2 have a severe effect on splicing (Madhani & Guthrie, 1994a).

The presence of the same interaction in vivo and in a protein-free complex assembled in vitro proves that the proximity of the two regions in the annealed U2-U6 complex is dictated by the primary structure of the two RNA molecules, and so the formation of this interaction seems to be an inherent property of the U2-U6 complex. Given the high efficiency of formation of the crosslinked species, it is conceivable that in the spliceosome the U2-U6 base-paired complex might also be able to fold properly without the help of proteins, although the interaction may be controlled, stabilized, or fine-tuned by spliceosomal proteins. The potential significance of this crosslink is enhanced by its ability to bring together the phosphate oxygens known to be important in catalysis of splicing (Fig. 1), probably helping to create metal-binding pockets in the active site.

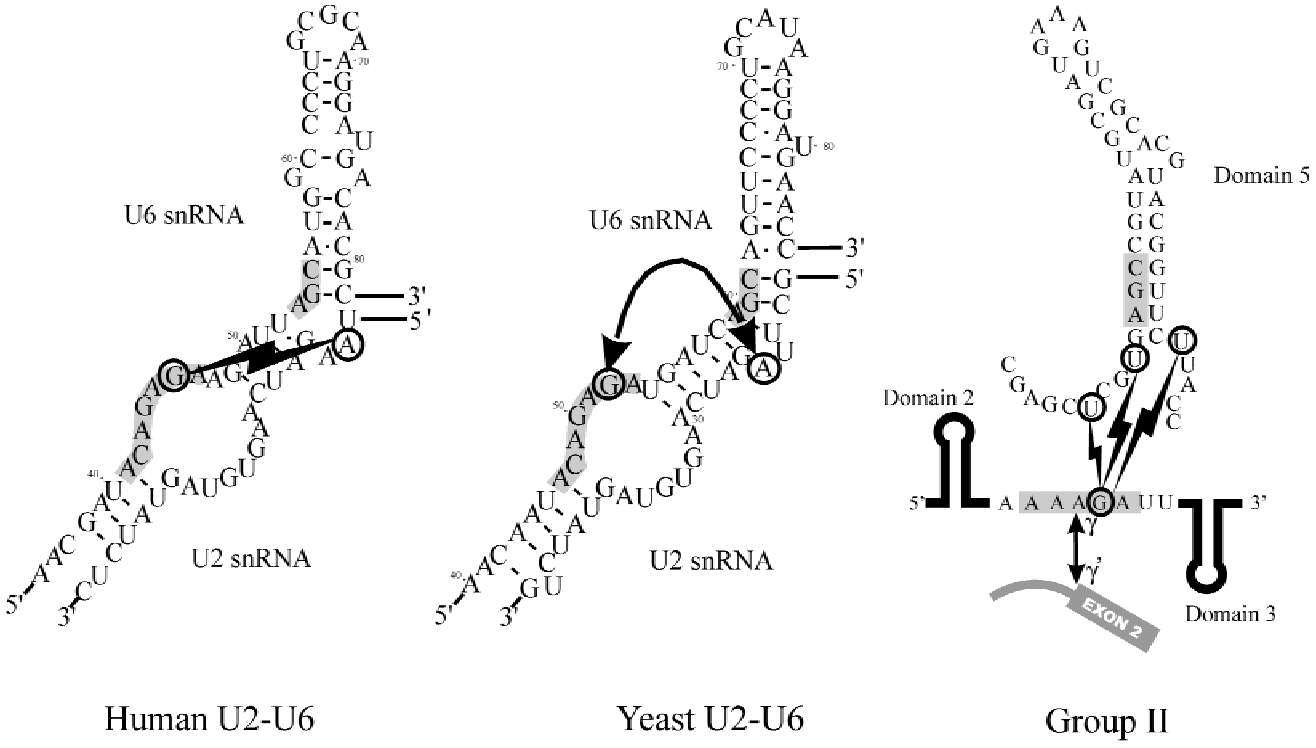

FIGURE 8. Similarities between tertiary interactions observed in human, yeast and group II splicing. **Left**: A model for the interaction observed in the U2-U6 major crosslinked species. **Center**: A tertiary interaction described in yeast in a genetic covariation-suppression study (Madhani & Guthrie, 1994a). **Right**: The crosslinkable interaction observed in group II introns (Podar et al., 1998). The ACAGAGA and AGC boxes and their group II analogues are shaded in gray. The nucleotides involved in crosslinking or genetic interaction are marked by circles and connected. The γ-γ' interaction in group II introns is shown by an arrow and labeled. Locations of U2 and U6 snRNAs and domains 2, 3, and 5 of group II introns are indicated.

Parallels between the interactions in the spliceosomal and group II active sites?

A 4-thio U-induced crosslink described in group II introns between the conserved AAA**G**A sequence located between domains 2 and 3 of the intron and U residues in the vicinity of the AGC sequence at the base of domain 5 (Podar et al., 1998) also bears striking resemblance to the crosslink we obtained in the U2-U6 annealed complex (see Fig. 8). One of the nucleotides in the AA**A**GA sequence in group II introns, the γ A, is involved in an interaction with the 3′ splice site (γ–γ' interaction), which is known to be important in the second step of splicing (Jacquier & Michel, 1990; Jacquier & Jacquesson-Breuleux, 1991). G46 in the ACAGA**G**A sequence is similarly involved in an interaction with the 3′ splice site (Lesser & Guthrie, 1993). The proximity of these two analogous regions to the AGC sequence, which is critical for catalysis in both systems, suggests an interesting parallel in the organization of the active site in group II introns and the spliceosome. The crosslink in the group II introns can be detected both before and after the first step of splicing, providing proof that the two regions are located close during both catalytic steps. The high efficiency of the crosslink obtained in the U2-U6 annealed complex makes it possible that the two regions are held close throughout splicing as an intrinsic property of the base-paired RNA structure.

The long range U2-U6 interaction is not disrupted by mutations in the residues involved

The interaction we detected by UV crosslinking did not depend on the identity of the base located at position 46 of U6, at least in the case of the G46A mutant, in which the site of the crosslink was located adjacent to the wild-type site, probably resulting from an interaction similar to the wild type. Interestingly, the crosslinkable interaction in group II introns (see above) is also very tolerant of mutations in the nucleotides involved (Podar et al., 1998). The analysis of the crosslinks obtained from the other two mutants, G46C and G46U, is not informative due to the inherent limitation of the crosslinking approach, as the absence of an appropriate crosslink does not necessarily rule out the presence of the interaction in the complex. The effect of mutations on formation of the interaction in vivo is complicated by the critical role G46 plays in the second step of splicing. Although mutations in the 2-nt bulge of U2 are relatively well tolerated, with the only observable phenotype being an increase in splicing intermediates, G46 mutants cause a severe block to the second step of splicing (Madhani & Guthrie, 1992, 1994a). But these effects can result from loss of a critical interaction with the 5′ or 3′ splice site rather than impairment in the interaction between the two regions. Current data (McPheeters & Abelson, 1992; Madhani & Guthrie, 1994a) suggests that the interaction is very tolerant of mutations in the nucleotides involved, consistent with our data, and/or redundant with another interaction (see below).

A role for proteins in the spliceosomal active site?

The highly conserved U5-associated protein, U5 220-kDa (Prp8), important in both tri-snRNP formation and spliceosome assembly (Brown & Beggs, 1992), is currently the most likely protein to participate directly in catalysis. Prp8 has been implicated in interactions with both 5′ and 3′ splice sites, and the polypyrimidine tract (Teigelkamp et al., 1995a, 1995b; Umen & Guthrie, 1995; Reyes et al., 1996). Mutations in Prp8 have been shown to suppress mutations at the 5′ and 3′ splice sites, as well as mutations in the U6 ACAG**A**GA box and U4 snRNA (Collins & Guthrie, 1999; Kuhn et al., 1999; Siatecka et al., 1999), which may suggest a role for Prp8 as a general stabilizing element for RNA–RNA interactions in the spliceosome. Precedents for such roles for proteins in RNA-centric catalytic systems have been demonstrated for group I introns, RNase P, and the hammerhead ribozyme (Guerrier-Takada et al., 1983; Tsuchihashi et al., 1993; Weeks & Cech, 1995). The fact that U5, and Prp8, are involved in splicing of both U2-dependent and U12-dependent introns indicates that the function of Prp8 does not depend on the identity of nucleotides at the splice junctions (Tarn & Steitz, 1996; Luo et al., 1999). Alternatively, the apparent lack of specificity might result from redundancy with another spliceosomal component; for example, the function of loop I of U5 can be fulfilled by other U5-associated components, probably Prp8, which in fact has an interaction pattern with splice sites similar to that of loop I (O'Keefe et al., 1996; Segault et al., 1999).

Two overlapping RNA–RNA interaction networks in the spliceosome

Our results and the currently available data point to two partially redundant RNA–RNA interaction networks in the active site of the spliceosome. The interactions between U6 G46 and the 3′ and 5′ splice sites are stabilized, we suggest, by an interaction between these three RNA elements and the U5 loop I–Prp8 complex. The interaction between G46 and the 2-nt bulge of U2, which also interacts with both 5′ and 3′ splice sites, could further stabilize the interactions between U6 and the splice sites. The interaction between G46 and the U2 bulge also likely helps keep the ACAGAGA box close to the AGC sequence, positioning the phosphate oxygens 5′ of A45 and A53 at the correct position for catalysis. Mutations in the 2-nt bulge of U2 normally do

not have a severe phenotype, as the interactions will be largely maintained by the other stabilizing interactions with U5. But when the G46–U5 interaction is compromised by mutations in loop I of U5 or G46 of U6, the stabilizing effect of the U2-U6 interaction becomes critical for proper placement of the reactive groups. The above model can also explain the synthetic lethality of mutations in the nucleotides immediately upstream of the U2 bulge with mutations in U5 loop I (Xu et al., 1998). As both these regions are involved in interactions with the 3′ splice site, it is conceivable that weakening these interactions would lead to a serious defect in positioning the 3′ splice site in the active site of the spliceosome.

We believe that the U2-U6 complex described here provides an attractive, albeit undoubtedly oversimplified, model for U2-U6 interactions in the spliceosome. Importantly, our results prove that at least some of the interactions in the active site of the spliceosome can result from the inherent folding ability of the RNA molecules involved. The RNA–RNA interactions between the 5′ splice site and the branch site with the ACAG AGA sequence in U6 and the branch-binding site of U2, respectively, help to bring the reactants involved in the first step of splicing together. The interaction described in this study, together with previous data, provides a means by which the same two snRNAs can both position residues involved in forming the active site, and also help bring together the reactants for the second catalytic step.

MATERIALS AND METHODS

RNA transcription and end labeling

All U2 and U6 snRNA fragments were transcribed from DNA templates that were amplified by PCR on a U6 or U2-containing plasmid by 5′-overhanging primers containing the sequence of the T7 promoter region, using bacteriophage T7 RNA polymerase. The amplified PCR products contained U2 sequences 1–54 and U6 sequences 25–99 in addition to T7 promoter sequences. All RNAs were purified from a 20% denaturing polyacrylamide gel in Tris-borate-EDTA buffer, eluted by diffusion and precipitated. RNAs were 5′-end labeled with [γ-^{32}P] ATP and T4 polynucleotide kinase following dephosphorylation with calf intestinal phosphatase, or 3′-end labeled with [5′-^{32}P] pCp and T4 RNA ligase.

Annealing of U2 and U6

Purified U2 and U6 were mixed in a buffer containing different concentrations of Mg^{2+} or other cations and 40 mM Tris, pH 6.8–7.2, at concentrations ranging from 1 nM to 1.2 μM. A typical annealing reaction contained 100 nM of the unlabeled RNA and 10 nM of the labeled RNA. The reaction was heated to 70 °C and cooled down very slowly to room temperature over about 1.5 h, although heating the RNAs to any temperature above 60 °C would result in complex formation (results not shown). For analyzing complex formation, reaction mixtures were loaded on an 8% nondenaturing PAGE in Tris-borate-EDTA buffer and run at 140 mV for 5–8 h in the 4 °C room after 1 h of prerunning.

UV crosslinking

Reaction mixtures containing the annealed RNAs were placed into wells of a Falcon 96-well microtiter plate resting on ice. Samples were irradiated for 5-min intervals for up to 60 min total, interrupted by 5-min periods to prevent overheating. Irradiation was done with a hand-held 254-nm UV light (model FB-UVLS-80, from Fisherbiotech, intensity at 15 cm: 650 μW/cm^2) at a distance of 1 cm. Recently, we have obtained comparable efficiencies of crosslinking in 5 min total irradiation using a Stratalinker UV crosslinker (Stratagene, model 1800). After crosslinking, RNAs were analyzed by 12% denaturing PAGE. For mapping of the crosslinked nucleotides, the crosslinked products were visualized by autoradiography, excised from the gel, eluted by diffusion, extracted, and precipitated. Quantitation of crosslinking was done using a Storm Phosphorimager (Molecular Dynamics).

RNase H digestion and primer extension reactions

DNA oligonucleotides used in RNase H digestion assays were complementary to nt 25–42, 37–55, 50–71, 67–82, and 82–99 of human U6 and 1–20, 14–36, 28–42, and 36–54 of human U2. The crosslinked products were annealed to the oligos at a final oligo concentration of approximately 8 μM by heating to 80 °C and cooling slowly to room temperature. The reaction was performed in a buffer containing 100 mM KCl, 50 mM $MgCl_2$, 100 mM Tris-HCl, pH 7.5, 0.5 mM EDTA, 0.5 mM DTT, after the addition of 0.1–0.5 U of RNase H (Amersham Pharmacia). Reaction mixtures were incubated at 30–37 °C for 2–30 min (different for each oligo) and then loaded directly onto a 12% denaturing gel along with similar reactions performed on uncrosslinked RNAs as control.

For primer extension reactions, the crosslinked products were annealed to a fivefold molar excess of an oligo complementary to the 3′ end (nt 82–99) of U6 by heating to 70 °C and cooling gradually to room temperature. After the addition of 1 U AMV reverse transcriptase (Promega), primer extension was performed in a buffer containing 50 mM Tris-HCl, pH 8.3, 50 mM KCl, 10 mM $MgCl_2$, 0.5 mM spermidine, and 10 mM DTT at 42 °C for 30–45 min. Reactions were terminated by addition of 10 μL formamide buffer (80% v/v formamide, 10 mM EDTA, and dyes) and denatured at 90 °C for 3 min before loading on a 20% denaturing PAGE along with sequencing reactions.

Mapping of crosslinked nucleotides

Gel-purified, end-labeled crosslinked products were subjected to limited alkaline hydrolysis. Samples were dissolved in 50 mM Na_3PO_4 buffer, pH 12.0, heated to 90 °C for 3–5 min, and loaded directly onto a 20% denaturing polyacrylamide gel. Noncrosslinked RNAs were similarly treated for 1–2 min and used as controls. RNase T1 reactions were performed on uncrosslinked RNAs in a buffer containing 8.5 mM sodium

citrate, pH 5.0, 2.6 M urea, and 0.4 mM EDTA, at 55 °C for 1–3 min after addition of 1 U RNase T1, and loaded along with the crosslinked samples.

ACKNOWLEDGMENTS

We thank Roland Tacke and Yoshio Takagaki for helpful discussion and suggestions. This work was supported by National Institutes of Health grant R37 GM 48259.

Received October 7, 1999; returned for revision November 4, 1999; revised manuscript received November 12, 1999

REFERENCES

Boulanger SC, Belcher SM, Schmidt U, Dib-Hajj SD, Schmidt T, Perlman PS. 1995. Studies of point mutants define three essential paired nucleotides in the domain V substructure of a group II intron. *Mol Cell Biol 15*:4479–4488.

Brow DA, Vidaver RM. 1995. An element in human U6 RNA destabilizes the U4/U6 spliceosomal RNA complex. *RNA 1*:122–131.

Brown JD, Beggs JD. 1992. Roles of PRP8 protein in the assembly of splicing complexes. *EMBO J 11*:3721–3729.

Burge CB, Tuschl T, Sharp PA. 1999. Splicing of precursors to mRNAs by the spliceosomes. In: Gesteland RF, Cech TR, Atkins JF, eds. *The RNA world.* Cold Spring Harbor, New York: Cold Spring Harbor Laboratory Press. pp 525–560.

Chanfreau G, Jacquier A. 1994. Catalytic site components common to both splicing steps of a group II intron. *Science 266*:1383–1387.

Chanfreau G, Jacquier A. 1996. An RNA conformational change between the two chemical steps of group II self-splicing. *EMBO J 15*:3466–3476.

Collins CA, Guthrie C. 1999. Allele-specific genetic interactions between prp8 and RNA active site residues suggest a function for prp8 at the catalytic core of the spliceosome. *Genes & Dev 13*:1970–1982.

Datta B, Weiner AM. 1991. Genetic evidence for base pairing between U2 and U6 snRNA in mammalian mRNA splicing. *Nature 352*:821–824.

Fabrizio P, Abelson J. 1990. Two domains of yeast U6 small nuclear RNA required for both steps of nuclear precursor messenger RNA splicing. *Science 250*:404–409.

Fabrizio P, Abelson J. 1992. Thiophosphates in yeast U6 snRNA specifically affect pre-mRNA splicing in vitro. *Nucleic Acids Res 20*:3659–3664.

Field DJ, Friesen JD. 1996. Functionally redundant interactions between U2 and U6 spliceosomal snRNAs. *Genes & Dev 10*:489–501.

Fortner DM, Troy RG, Brow DA. 1994. A stem/loop in U6 RNA defines a conformational switch required for pre-mRNA splicing. *Genes & Dev 8*:221–233.

Guerrier-Takada C, Gardiner K, Marsh T, Pace N, Altman S. 1983. The RNA moiety of ribonuclease P is the catalytic subunit of the enzyme. *Cell 35*:849–857.

Hausner TP, Giglio LM, Weiner AM. 1990. Evidence for base-pairing between mammalian U2 and U6 small nuclear ribonucleoprotein particles. *Genes & Dev 4*:2146–2156.

Hetzer M, Wurzer G, Schweyen RJ, Mueller MW. 1997. *Trans*-activation of group II intron splicing by nuclear U5 snRNA. *Nature 386*:417–420.

Jacquier A, Jacquesson-Breuleux N. 1991. Splice site selection and role of the lariat in a group II intron. *J Mol Biol 219*:415–428.

Jacquier A, Michel F. 1990. Base-pairing interactions involving the 5′ and 3′-terminal nucleotides of group II self-splicing introns. *J Mol Biol 213*:437–447.

Kambach C, Walke S, Nagai K. 1999. Structures and assembly of the spliceosomal small nuclear ribonucleoprotein particles. *Curr Opin Struc Biol 9*:222–230.

Kim CH, Abelson J. 1996. Site-specific crosslinks of yeast U6 snRNA to the pre-mRNA near the 5′ splice site. *RNA 2*:995–1010.

Kramer A. 1996. The structure and function of proteins involved in mammalian pre-mRNA splicing. *Annu Rev Biochem 65*:367–409.

Kuhn AN, Li Z, Brow DA. 1999. Splicing factor Prp8 governs U4/U6 RNA unwinding during activation of the spliceosome. *Mol Cell 3*:65–75.

Lesser CF, Guthrie C. 1993. Mutations in U6 snRNA that alter splice site specificity: Implications for the active site. *Science 262*:1982–1988.

Luo HR, Moreau GA, Levin N, Moore MJ. 1999. The human Prp8 protein is a component of both U2- and U12-dependent spliceosomes. *RNA 5*:893–908.

Luukkonen BGM, Séraphin B. 1998a. Genetic interaction between U6 snRNA and the first intron nucleotide in *Saccharomyces cerevisiae*. *RNA 4*:167–180.

Luukkonen BGM, Séraphin B. 1998b. A role for U2/U6 helix Ib in 5′ splice site selection. *RNA 4*:915–927.

Madhani HD, Bordonne R, Guthrie C. 1990. Multiple roles for U6 snRNA in the splicing pathway. *Genes & Dev 4*:2264–2277.

Madhani HD, Guthrie C. 1992. A novel base-pairing interaction between U2 and U6 snRNAs suggests a mechanism for the catalytic activation of the spliceosome. *Cell 71*:803–817.

Madhani HD, Guthrie C. 1994a. Randomization-selection analysis of snRNAs in vivo: Evidence for a tertiary interaction in the spliceosome. *Genes & Dev 8*:1071–1086.

Madhani HD, Guthrie C. 1994b. Dynamic RNA–RNA interactions in the spliceosome. *Annu Rev Genet 28*:1–26.

McPheeters DS, Abelson J. 1992. Mutational analysis of the yeast U2 snRNA suggests a structural similarity to the catalytic core of group I introns. *Cell 71*:819–831.

Newman AJ, Teigelkamp S, Beggs JD. 1995. snRNA interactions at 5′ and 3′ splice sites monitored by photoactivated crosslinking in yeast spliceosomes. *RNA 1*:968–980.

Nilsen TW. 1998. RNA–RNA interactions in nuclear pre-mRNA splicing. In: Simons R, Grunberg-Manago M, eds. *RNA structure and function*. Cold Spring Harbor, New York: Cold Spring Harbor Laboratory Press. pp 279–307.

O'Keefe RT, Norman C, Newman AJ. 1996. The invariant U5 snRNA loop 1 sequence is dispensable for the first catalytic step of pre-mRNA splicing in yeast. *Cell 86*:679–689.

Parker R, Siliciano PG. 1993. Evidence for an essential non-Watson–Crick interaction between the first and last nucleotides of a nuclear pre-mRNA intron. *Nature 361*:660–662.

Peebles CL, Zhang M, Perlman PS, Franzen JS. 1995. Catalytically critical nucleotides in domain V of a group II intron. *Proc Natl Acad Sci USA 92*:4422–4426.

Podar M, Perlman PS. 1999. Photocrosslinking of 4-thio uracil-containing RNAs supports a side-by-side arrangement of domains 5 and 6 of a group II intron. *RNA 5*:318–329.

Podar M, Zhuo J, Zhang M, Franzen JS, Perlman PS, Peebles CL. 1998. Domain 5 binds near a highly conserved dinucleotide in the joiner linking domains 2 and 3 of a group II intron. *RNA 4*:151–166.

Reyes JL, Kois P, Konforti BB, Konarska MM. 1996. The canonical GU dinucleotide at the 5′ splice site is recognized by p220 of the U5 snRNP within the spliceosome. *RNA 2*:213–225.

Segault V, Will CL, Polycarpou-Schwarz M, Mattaj IW, Branlant C, Lührmann R. 1999. Conserved loop I of U5 small nuclear RNA is dispensable for both catalytic steps of pre-mRNA splicing in HeLa nuclear extracts. *Mol Cell Biol 19*:2782–2790.

Siatecka M, Reyes JL, Konarska MM. 1999. Functional interactions of prp8 with both splice sites at the spliceosomal catalytic center. *Genes & Dev 13*:1983–1993.

Sontheimer EJ, Gordon PM, Piccirilli JA. 1999. Metal ion catalysis during group II intron self-splicing: Parallels with the spliceosome. *Genes & Dev 13*:1729–1741.

Sontheimer EJ, Steitz JA. 1993. The U5 and U6 small nuclear RNAs as active site components of the spliceosome. *Science 262*:1989–1996.

Sontheimer EJ, Sun S, Piccirilli JA. 1997. Metal ion catalysis during splicing of pre-messenger RNA. *Nature 388*:801–805.

Staley JP, Guthrie C. 1998. Mechanical devices of the spliceosome: Motors, clocks, springs, and things. *Cell 92*:315–326.

Steitz TS, Steitz JA. 1993. A general two-metal-ion mechanism for catalytic RNA. *Proc Natl Acad Sci USA 90*:6498–6502.

Sun J, Manley JL. 1995. A novel U2-U6 snRNA structure is necessary for mammalian mRNA splicing. *Genes & Dev 9*:843–854.

Sun J, Valadkhan S, Manley JL. 1998. A UV-crosslinkable interaction in human U6 snRNA. *RNA 4*:489–497.

Tarn WY, Steitz JA. 1996. A novel spliceosome containing U11, U12 and U5 snRNPs excises a minor class (AT-AC) intron in vitro. *Cell 84*:801–811.

Teigelkamp S, Newman AJ, Beggs JD. 1995a. Extensive interactions of PRP8 protein with the 5′ and 3′ splice sites during splicing suggest a role in stabilization of exon alignment by U5 snRNA. *EMBO J 14*:2602–2612.

Teigelkamp S, Whitaker E, Beggs JD. 1995b. Interaction of the yeast splicing factor Prp8 with substrate RNA during both steps of splicing. *Nucleic Acids Res 23*:320–326.

Tsuchihashi Z, Khosla M, Herschlag D. 1993. Protein enhancement of hammerhead ribozyme catalysis. *Science 262*:99–102.

Tuschl T, Sharp PA, Bartel DP. 1998. Selection in vitro of novel ribozymes from a partially randomized U2 and U6 snRNA library. *EMBO J 17*:2637–2650.

Umen JG, Guthrie C. 1995. A novel role for a U5 snRNP protein in 3′ splice site selection. *Genes & Dev 9*:855–868.

Weeks KM, Cech TR. 1995. Protein facilitation of group I intron splicing by assembly of the catalytic core and the 5′ splice site domain. *Cell 82*:221–230.

Wolff T, Bindereif A. 1992. Reconstituted mammalian U4/U6 snRNP complements splicing: A mutational analysis. *EMBO J 11*:345–359.

Wolff T, Menssen R, Hammel J, Bindereif A. 1994. Splicing function of mammalian U6 small nuclear RNA: Conserved positions in central domain and helix I are essential during the first and second step of pre-mRNA splicing. *Proc Natl Acad Sci USA 91*:903–907.

Wu J, Manley JL. 1991. Base pairing between U2 and U6 snRNAs is necessary for splicing of a mammalian pre-mRNA. *Nature 352*: 818–821.

Xu D, Field DJ, Tang S, Moris A, Bobechko BP, Friesen JD. 1998. Synthetic lethality of yeast slt mutations with U2 small nuclear RNA mutations suggests functional interactions between U2 and U5 snRNPs that are important for both steps of pre-mRNA splicing. *Mol Cell Biol 18*:2055–2066.

Yan D, Ares M. 1996. Invariant U2 RNA sequences bordering the branchpoint recognition region are essential for interaction with yeast SF3a and SF3b subunits. *Mol Cell Biol 16*:818–828.

Yu Y, Maroney PA, Darzynkiewicz E, Nilsen TW. 1995. U6 snRNA function in nuclear pre-mRNA splicing: A phosphorothioate interference analysis of the U6 phosphate backbone. *RNA 1*: 46–54.